Frequency-Domain Detection of OQPSK Signals with Quasi-Constant Envelope and High Spectral Efficiency

M. Serrazina(1), R.Dinis(2) and P.Carvalho(1)
(1) UNINOVA, FCT-UNL, Monte da Caparica, Portugal
(2) ISR-IST, Tech. Univ. of Lisbon, Portugal

Abstract - In this paper, we consider SC-FDE schemes (Single Carrier with Frequency-Domain Equalization) employing OQPSK (Offset Quaternary Phase Shift Keying) signals with quasi-constant envelope. To allow high spectral efficiency, different frequency channels are separated by the symbol rate, regardless of their bandwidth (which is much higher than the symbol rate for quasi-constant envelope OQPSK signals), and we consider a multi-channel frequency-domain receiver with ACI (Adjacent Channel Interference) suppression.

Our performance results show that it is possible to have high spectral efficiency with quasi-constant envelope OQPSK signals. This technique is especially interesting for the uplink of future broadband wireless systems since we can employ low-cost, grossly nonlinear power amplifiers at the mobile terminals and almost all signal processing is shifted to the base station.[1]

Index Terms: OQPSK signals, frequency domain equalization, ACI suppression, multiuser detection.

I. Introduction

It is well-known that an efficient and low-cost power amplification is very important at the mobile terminal. For this reason, single-carrier modulations with frequency domain equalization (usually denoted by SC-FDE) have been recommended for the uplink of broadband wireless systems [1], [2]. In fact, since the envelope fluctuations of SC-FDE signals are relatively low (much lower than with multicarrier signals), they allow an efficient power amplification. However, the dynamic range of the envelope is relatively high, with frequent zero crossing, when spectral efficient modulations are employed (e.g., for a square-root raised cosine filtering), even for constant envelope PSK constellations. This means that a linear amplifier (although with reduced backoff) is required at the transmitter.

Grossly nonlinear amplifiers have higher amplification efficiency and output power and are cheaper than linear amplifiers. However, these amplifiers are only recommendable if the signal at its input has an almost constant envelope. These amplifiers are usually employed with OQPSK-type signals (Offset Quaternary Phase Shift Keying), which can have very low envelope fluctuations or even a constant envelope (e.g., for MSK signals (Minimum Shift Keying)).

The major problem with OQPSK signals with very low envelope fluctuations is that their bandwidth is much higher than the symbol rate. If we do not want to have ACI (Adjacent Channel Interference) the separation between frequency channels should be much higher than the symbol rate, reducing the spectral efficiency of the modulation. A promising technique was proposed in [3] for QPSK signals where the separation between frequency channels is equal to the symbol rate, regardless of the transmission bandwidth associated to each channel. To cope with the high interference levels that can result form having significant overlap between adjacent channels an iterative frequency-domain receiver with joint equalization and ACI suppression was proposed in [3]. That receiver takes advantage of spectral correlations for the separation of cyclostationary signals [4], [5], [6] and allows excellent performance.

In this paper, we consider the extension of the receiver proposed in [3] to OQPSK-type signals with very low envelope fluctuations. We consider different OQPSK-type signals with quasi-constant envelope and different complexity/performance tradeoffs.

This paper is organized as follows. The system characterization is made in sec. II and sec. III presents several OQPSK signals with reduced envelope fluctuations. Sec. IV describes the receiver structure and a set of performance results is presented in sec. V. Sec. VI concludes the paper.

II. System Description and Transmitted Signals

In this paper we consider an FDMA (Frequency Division Multiple Access) system where an SC-FDE modulation is employed for each frequency channel. We have frequency P channels (see fig. 1), with the carrier frequency of the pth channel denoted by f_p, $p = 1, 2, \ldots, P$, with $f_p - f_{p-1} = \Delta f$ (i.e., the frequency channels are equally spaced) and the blocks transmitted by each frequency channel have the same dimensions.

The length-M data block to be transmitted by the pth channel is $\{a_{m,p}; m = 0, 1, \ldots, M-1$, where $a_{m,p} = a_{m,p}^{(I)} + j a_{m,p}^{(Q)}$

[1]This work was partially supported by the FCT (plurianual funding and project POSI/CPS/46701/2002 - MC-CDMA).

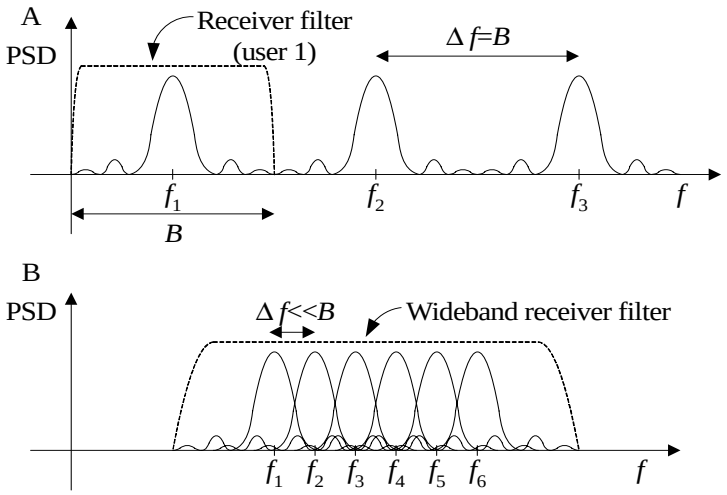

Fig. 1. PSD of the signals without ACI (A) or with ACI (B).

is the mth data symbol, where $a_{m,p}^{(I)} = \text{Re}\{a_{m,p}\} = \pm 1$ and $a_{m,p}^{(Q)} = \text{Im}\{a_{m,p}\} = \pm 1$. The corresponding signal is

$$s_p(t) = \sum_{m=-M_G}^{M-1} a_{m,p}^{(I)} h_T(t - mT_S) + \\ + \sum_{m=-M_G}^{M-1} j a_{m,p}^{(Q)} h_T(t - mT_S - \Delta T_S), \quad (1)$$

with T_S denoting the symbol duration, M_G denoting the number of samples at the CP (Cyclic Prefix) (it is assumed that $a_{-m,p} = a_{M-m,p}$) and $h_T(t)$ is the transmitted pulse shaping filter response. (1) corresponds to a QPSK signal for $\Delta T_S = 0$ and an OQPSK signal for $\Delta T_S = T_S/2$. in this paper we consider OQPSK-type signals, i.e., $\Delta T_S = T_S/2$.

Let us consider now the sampled version of the useful part of $s_(t)$ with sampling ratio J/T_S, i.e., the samples $s_{n,p} \triangleq s_p(nT_S/J)$. Clearly, $\{s_{n,p}; n = 0, 1, \ldots, JM-1\}$ is the cyclic convolution between $\{h_{T,n}; n = 0, 1, \ldots, JM-1\}$ and $\{p_{n,p}; n = 0, 1, \ldots, JM-1\}$, with $h_{T,n}$ denoting the sampled version of $h_T(t)$ and $p_n = a_{m,p}^{(I)}$ for $n = mJ$, $p_n = a_{m,p}^{(Q)}$ for $n = mJ + J/2$ and p_n, otherwise. This means that the DFT (Discrete Fourier Transform) of $\{s_{n,p}; n = 0, 1, \ldots, JM-1\}$ is $\{S_{k,p} = H_{T,k} P_{k,p}; k = 0, 1, \ldots, JM-1\}$, with $\{H_{T,k}; k = 0, 1, \ldots, JM-1\}$ = DFT $\{h_{T,n}; n = 0, 1, \ldots, JM-1\}$ and $\{P_{k,p}; k = 0, 1, \ldots, JM-1\}$ = DFT $\{p_{n,p}; n = 0, 1, \ldots, JM-1\}$. It can easily be shown that

$$P_{k+lM,p} = \frac{A_{k,p}^{(I)} + j A_{k,p}^{(Q)} \Theta_k (-1)^l}{L} \quad (2)$$

($k = 0, 1, \ldots, M-1$), with $\{A_{k,p}^{(I)}; k = 0, 1, \ldots, JM-1\}$ = DFT $\{a_{n,p}^{(I)}; n = 0, 1, \ldots, JM-1\}$, $\{A_{k,p}^{(Q)}; k = 0, 1, \ldots, JM-1\}$ = DFT $\{a_{n,p}^{(Q)}; n = 0, 1, \ldots, JM-1\}$ and $\Theta_k = \exp(-j\pi k/M)$. Clearly, $\{A_{k,p} = A_{k,p}^{(I)} + j A_{k,p}^{(Q)}; k = 0, 1, \ldots, JM-1\}$ = DFT $\{a_{n,p} = a_{n,p}^{(I)} + j a_{n,p}^{(Q)}; n = 0, 1, \ldots, JM-1\}$[2]. This means that when there is a multiplicity in the frequency-domain samples $A_{k,p}^{(I)}$ and $A_{k,p}^{(Q)}$ whenever the bandwidtrh of $h_T(t)$ is larger than $R_S = 1/T_S$ (see fig. 2). This multiplicity, which is associated to the cyclostationary nature of the transmitted signals, can be used for signal separation in the presence of ACI [3].

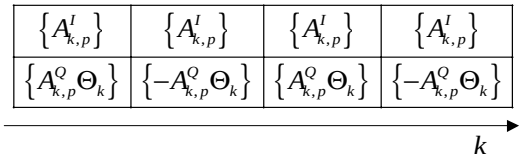

Fig. 2. Multiplicity in the frequency-domain samples $A_{k,p}^{(I)}$ and $A_{k,p}^{(Q)}$ for OQPSK signals.

III. Pulse Sphapping for Quasi-Constant Envelope Signals

The most common option with respect to $h_T(t)$ is to adopt a square-root raised-cosine filtering with a given roll-off factor β. For an ideal AWGN channel this allows zero ISI (Inter-Symbol Interference) at the matched filter output, together with compact spectrum, since the bandwidth of $s_p(t)$ is $B = (1+\beta)R_S$ (the minimum bandwidth for ISI-free transmission is $R_S = 1/T_S$, i.e., the symbol rate). The major problem is that the transmitted signals have relatively high envelope fluctuations, especially for smaller values of β (i.e., when the spectrum is more compact), as shown in fig. 3; for OQPSK schemes the dynamic range of the envelope is much lower for OQPSK signals since there are no zero crossings.

However, if grossly nonlinear power amplifiers are employed then the signal at its input should have constant envelope. If not, the nonlinear nature of the power amplifier distorts the signals, leading to spectral widening and performance degradation. This means that a square-root raised-cosine filtering is not suitable, even for OQPSK schemes. In that case, we can employ MSK signals, which can be regarded as constant-envelope OQPSK signals where

$$h_T(t) = \cos\left(\frac{\pi t}{T_S}\right) \text{rect}\left(\frac{t}{T_S}\right). \quad (3)$$

The major problem associated to MSK signals is that they have very large bandwidth. To reduce the spectral MSK signals can be filtered, although this leads to some regrowth in the envelope fluctuations, as shown in table I, where two cases are considered: rectangular filtering $H_F(f) = \text{rect}(f/B_T)$ and Gaussian $H_F(f) = \exp(-f^2/B_T^2/2)$.

Naturally, we do not need to restrict to MSK-type pulses. For instance, we could adopt the modified pulse shape

$$h_T(t) = \frac{1}{2}\text{rect}\left(\frac{t}{2T_S}\right)\left(\cos^2\left(\frac{\pi t}{T_S}\right) + \cos\left(\frac{\pi t}{T_S}\right)\right), \quad (4)$$

[2]It should be pointed out that $A_{k,p}^{(I)}$ and $A_{k,p}^{(Q)}$ are not necessarily the real and imaginary parts of $A_{k,p}$.

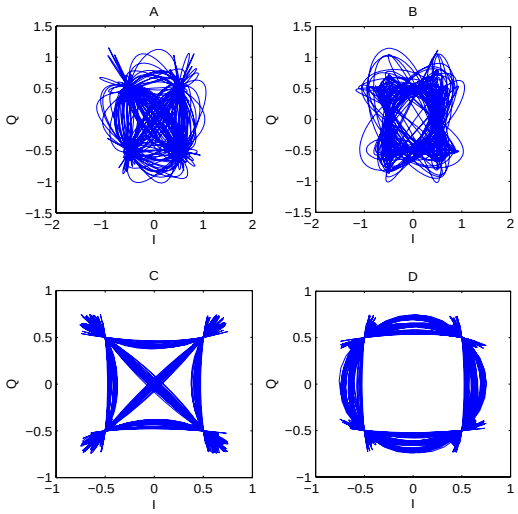

Fig. 3. I-Q diagram when a square-root raised-cosine filtering with roll-off β is adopted, for QPSK schemes ((A) for $\beta = 0.0$ and (B) for $\beta = 1$) and OQPSK schemes ((A) for $\beta = 0.0$ and (B) for $\beta = 1$).

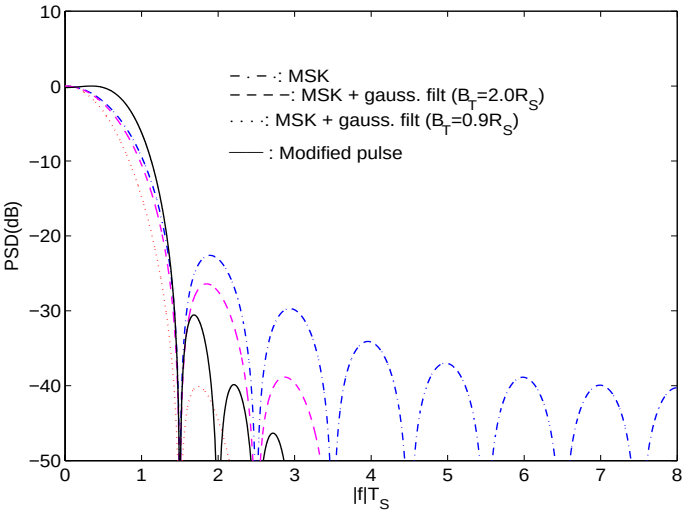

Fig. 5. PSD of the transmitted signals.

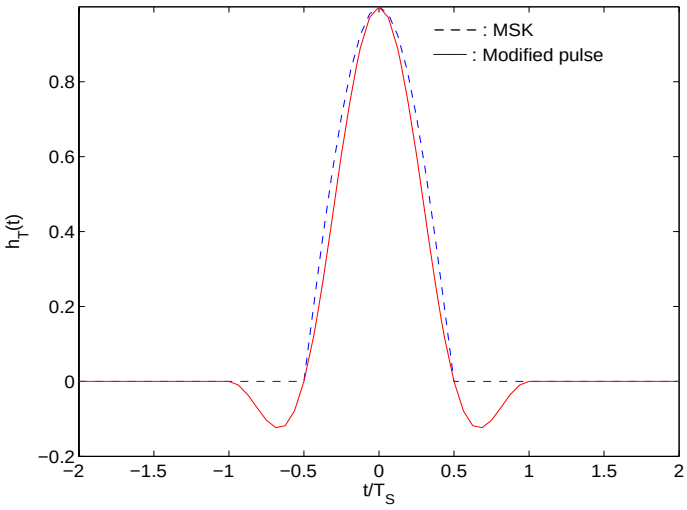

Fig. 4. Modifed pulse, together with ideal MSK pulse.

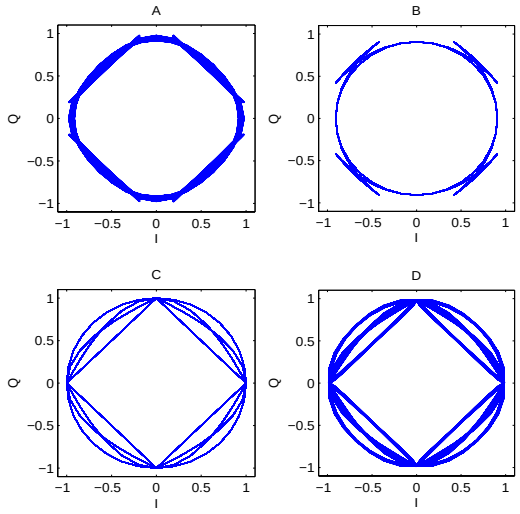

Fig. 6. I-Q diagram of the transmitted signals in the following cases: (A) MSK signals with rectangular filtering ($B_T = 3R_S$); (A) MSK signals with Gaussian filtering ($B_T = 0.9R_S$); (C) modified pulse of fig. 4; (C) modified pulse of fig. 4 with rectangular filtering ($B_T = 3R_S$).

depicted in fig. 4, which spectrum is more compact than the one of MSK signals, as shown in fig. 5. The cossesponding I-Q diagram are depicted in fig. 6; table II shows the PMEPR values when a rectangular filtering $H_F(f) = \text{rect}(f/B_T)$ is assumed.

However, quasi-constant envelope OQPSK signals with compact spectrum still have relatively high bandwidth, about 3 to 5 times the symbol rate R_S (i.e., the minimum bandwidth achieved with a square-root raised-cosine filtering with roll-off $\beta = 0.0$). To allow high spectral efficiencies the channel separation should be R_S, which leads to high ACI levels, precluding the separate detection of each frequency channel. In that case, we need to jointly detect all frequency channels, as proposed in [3] for QPSK signals. The receiver is described in sec. IV.

IV. Receiver Structure

We assume that $\Delta f = R_S < B$ (the extension to other cases is straightforward) and we consider a receiver based on the one proposed in [3]. We employ a wideband reception filter and the resulting signal is sampled with an oversampling factor J, large enough to avoid aliasing effects, leading to the time-domain received block $\{y_m; m = 0, 1, \ldots, JM-1\}$. The corresponding frequency-domain block, obtained after an appropriate size-JM DFT operation (Discrete Fourier Transform), is $\{Y_k; k = 0, 1, \ldots, JM-1\}$, where Y_k can be written

TABLE I

PMEPR of the transmitted signals for filtered MSK signals

Rectangular filter		Gaussian filter	
$B_T T_S$	PMEPR (dB)	$B_T T_S$	PMEPR (dB)
3.75	0.04	7	0.23
2.0	0.15	5	0.26
0.9	0.52	3	0.86

TABLE II

PMEPR of the transmitted signals for OQSPK signals with the pulse shape of fig. 4 and a rectangular filtering.

$B_T T_S$	PMEPR (dB)
∞	0.60
4	0.67
3	0.85

as

$$Y_k = \sum_{p=1}^{P} S_{k-\Delta M_p,p} H_{k,p} + N_k, \tag{5}$$

with $H_{k,p}$ denoting the overall channel frequency response for the kth frequency of the pth frequency channel, and N_k denoting the corresponding channel noise. ΔM_p is an appropriate circular shift accounting for the difference between the carrier frequency of the pth channel and the reference frequency of the local oscillator at the receiver.

We consider a frequency-domain iterative multichannel detection where each iteration consists of P detection stages, one for each frequency channel. For a given iteration, the receiver structure for the detection of the in-phase component of the pth channel is illustrated in fig. 7 (the extension to the quadrature component is straightforward). We have one length-JM frequency-domain feedforward filter and two sets of P length-M frequency-domain feedback filters, one set for the inphase components of the P channels and the other set to remove the residual part of the quadratures components of the P channels.[3] The receiver implementation can be further simplified since most feedforward and feedback coefficients are zero.

Let us consider the detection of the in-phase component of the pth user (the extension for the quadrature component is straightforward). Having in mind the multiplicity inherent to the transmitted signals (see fig. 2), it can easily be shown that the kth frequency-domain sample associated can be given by

$$\tilde{A}^I_{k,p} = \mathrm{Re}\left\{ \sum_{l=0}^{J-1} F_{k+lM+\Delta M_p,p} Y_{k+lM+\Delta M_p,p} - \right.$$
$$\left. - \sum_{p'=1}^{P} B^{IQ(p')}_{k,p} \overline{A}^Q_{k+\Delta M'_p,p'} - \sum_{p'=1}^{P} B^{(p')}_{k,p} \overline{A}^I_{k+\Delta M'_p,p'} \right\} \tag{6}$$

with the feedforward coefficients $F_{k,p}$ ($k = 0, 1, \ldots, JM-1$) and two sets of feedforward coefficients and $B^{(p')}_{k,p}$ ($k = 0, 1, \ldots, M-1$; $p = 1, 2, \ldots, P$) and $B^{IQ(p')}_{k,p}$ ($k = 0, 1, \ldots, M-1$; $p = 1, 2, \ldots, P$), the first to remove the residual in-phase interference and the second to remove the residual quadrature interference. The blocks $\{\overline{A}^I_{k,p'}; k = 0, 1, \ldots, M-1\}$ and $\{\overline{A}^Q_{k,p'}; k = 0, 1, \ldots, M-1\}$ are the DFTs of the blocks $\{\overline{a}^I_{m,p'}; m = 0, 1, \ldots, M-1\}$ and $\{\overline{a}^Q_{m,p'}; m = 0, 1, \ldots, M-1\}$, respectively. For OQPSK constellations the average in-phase and quadrature values conditioned to the latest FDE output are

$$\overline{a}^I_{m,p'} = \tanh\left(\frac{L^I_{m,p'}}{2}\right) \tag{7}$$

and

$$\overline{a}^Q_{m,p'} = \tanh\left(\frac{L^Q_{m,p'}}{2}\right), \tag{8}$$

with the LLR (Log-Likelihood Ratio) of the in-phase and quadrature bits given by

$$L^I_{m,p'} = \frac{2}{\sigma_i^2} \tilde{a}^I_{m,p'} \tag{9}$$

and

$$L^Q_{m,p'} = \frac{2}{\sigma_i^2} \tilde{a}^Q_{m,p'}, \tag{10}$$

respectively, where $\{\tilde{a}^I_{m,p'}; m = 0, 1, \ldots, M-1\}$ = IDFT $\{\tilde{A}^I_{k,p'}; k = 0, 1, \ldots, M-1\}$, $\{\tilde{a}^Q_{m,p'}; m = 0, 1, \ldots, M-1\}$

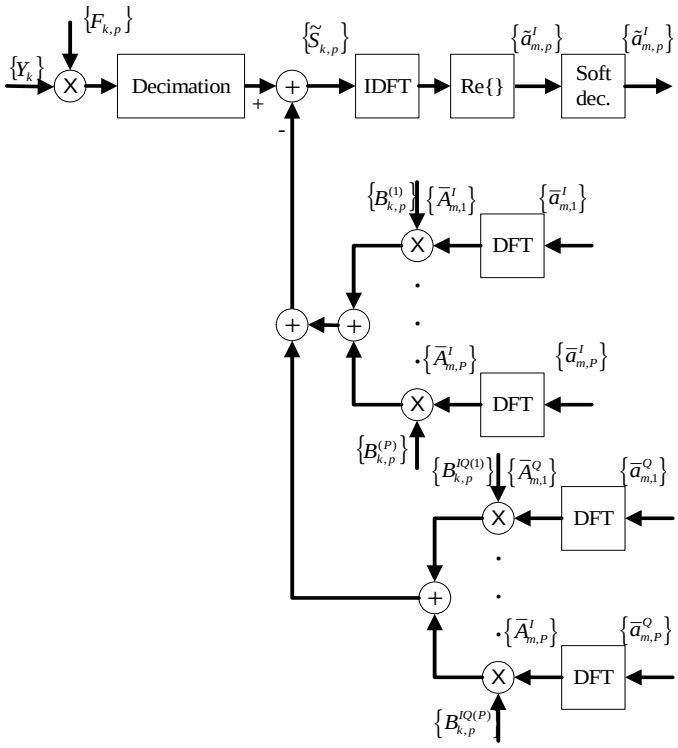

Fig. 7. Detection of the in-phase component of the pth frequency channel.

[3]Under ideal conditions it is not necessary to remove the quadrature components, since they would be imaginary at the sample instants of the in-phase components.

= IDFT $\{\tilde{A}^Q_{k,p'}; k = 0, 1, \ldots, M-1\}$ and

$$\sigma^2 = \frac{1}{2}(E[|a^I_{m,p'} - \tilde{a}^I_{m,p'}|^2] + E[|a^Q_{m,p'} - \tilde{a}^Q_{m,p'}|^2]) \approx$$
$$\approx \frac{1}{2M}\sum_{m=0}^{M-1}(|\hat{a}^I_{m,p'} - \tilde{a}^I_{m,p'}|^2 + |\hat{a}^Q_{m,p'} - \tilde{a}^Q_{m,p'}|^2), \quad (11)$$

with $\hat{a}^I_{m,p'}$ and $\hat{a}^Q_{m,p'}$ denoting the hard decisions associated to $\tilde{a}^I_{m,p'}$ and $\tilde{a}^Q_{m,p'}$, respectively.

The optimum feedforward coefficients can be written as and

$$F_{k,p} = \frac{\breve{F}_{k,p}}{\gamma_p}, \quad (12)$$

with

$$\gamma_p = \frac{1}{M}\sum_{l=0}^{J-1}\sum_{k=0}^{M-1}\breve{F}_{k+lM,p}H_{k+lM,p} \quad (13)$$

and $\breve{F}_{k+lM,p}$ ($l = 0, 1, \ldots, J-1$ and $k = 0, 1, \ldots, M-1$) obtained from the set of J equations:

$$(1-\rho_p^2)H^*_{k+lM,p}\sum_{l'=0}^{J-1}\breve{F}_{k+l'M,p}H_{k+l'M,p}$$
$$+\sum_{p'\neq p}(1-\rho^2_{p'})H^*_{k+lM,p'}\sum_{l'=0}^{J-1}\breve{F}_{k+l'M,p}H_{k+l'M,p'} +$$
$$+\frac{\breve{F}_{k-lM,p}}{SNR_p} = (1-\rho_p^2)H^*_{k-lM,p}, \quad l = 0, 1, \ldots, J-1, \quad (14)$$

where

$$SNR_p = \frac{E[|S_{k,p}|^2]}{E[|N_k|^2]} \quad (15)$$

and the correlation coefficient ρ_p is given by

$$\rho_p = \frac{1}{2M}\sum_{m=0}^{M-1}(|\overline{a}^I_{m,p'}| + |\overline{a}^Q_{m,p'}|). \quad (16)$$

The optimum feedback coefficients are

$$B^{(p)}_{k,p} = \sum_{l=0}^{J-1}F_{k+lM,p}H_{k+lM,p} - \delta_{p,p'} \quad (17)$$

($\delta_{p,p'} = 1$ for $p = p'$ and 0 for $p' \neq p$) and

$$B^{IQ(p)}_{k,p} = \sum_{l=0}^{J-1}F_{k+lM,p}H_{k+lM,p}\Theta_k(-1)^l. \quad (18)$$

Since $F_{k,p} = 0$ when $H_{k,p} = 0$, we just need to compute $MB/R_S)$ coefficients for each frequency channel and each iteration. (14) suggests that we need to solve a system of J equations for obtaining each feedforward coefficient. However, since the bandwidth of the transmitted signals associated to each frequency channel is B, the multiplicity of each $S_{k,p}$ is upper-bounded by $\lceil B/R_S \rceil$ ($\lceil x \rceil$ denotes "smaller integer greater than x"). Therefore, we just need to solve a system of $\lceil B/R_S \rceil$ equations for each of the M frequencies.

V. Performance Results

In this section we present a set of performance results concerning the proposed receiver for SC-FDE schemes with strong ACI levels. We consider the uplink transmission with $P = 5$ frequency channels, each one transmitting blocks of $M = 256$ data symbols (similar results were observed for other values of M, provided that $M >> 1$). We consider OQPSK employing filtered MSK-type pulses (both rectangular and Gaussian filtering, as described in sec. III), as well as the modified pulse shape (4) (also with rectangular filtering).

The propagation channel for each frequency channel is characterized by the power delay profile type C for the HIPERLAN/2 (HIgh PERformance Local Area Network) [8], with uncorrelated Rayleigh fading between frequency channels and on the different paths (similar results were observed for other strongly frequency-selective channels). The duration of the useful part of the data blocks (M symbols) is 4μs and the CP has duration 1.1μs. The power amplifier of each MT is assumed to be linear for the dynamic range of the signal at its input. Since this dynamic range is very small (less than 1dB, as shown in sec. III), grossly nonlinear power amplifiers can be employed. At the receiver, the average power associated to each frequency channel is the same. We assume perfect synchronization and channel estimation.

We employ the proposed receiver, with the frequency channels detected in a sequential order (i.e., for each iteration we detect first the frequency channel with lowest carrier frequency and proceed sequentially up to the frequency channel with highest frequency)[4]. For filtered MSK signals we need to solve a system of 3 or 5 equations for each frequency, depending on the adopted filter[5]; for the modified pulses (4) we need to solve a system of 3 or 4 equations for each frequency.

Fig. 8 shows the average BER, averaged over all channels, for MSK signals with rectangular filtering with $B_T = 3R_S$ (similar results were observed for other filters). We present both the performance without ACI ($\Delta f \geq B$) and the performance when $\Delta f = R_S$, allowing high spectral efficiency but with strong ACI levels. For the sake of comparisons, we included the MFB performance (Matched Filter Bound). Clearly, our receiver allows good ACI suppression, with performance close to the performance without ACI. Moreover, the BER can be close to the MFB after just three or four iterations.

Fig. 9, 10 and 11 show the average BER performance when $\Delta f = R_S$ and different pulses. Clearly we can efficiently separate different frequency channels, regardless of the adopted pulse shape. Naturally, different pulses lead to different envelope fluctuations on the transmitted signals. Moreover, the receiver complexity, which is associated to the bandwidth of the transmitted, might be different for different pulses.

[4]This sequential order is not necessarily optimal, since the channels with lowest interference levels should be detected first. However, after a few iterations the performance is almost the same regardless of the detection order.

[5]For Gaussian filters we considered only the lobes of the spectrum above -40dB.

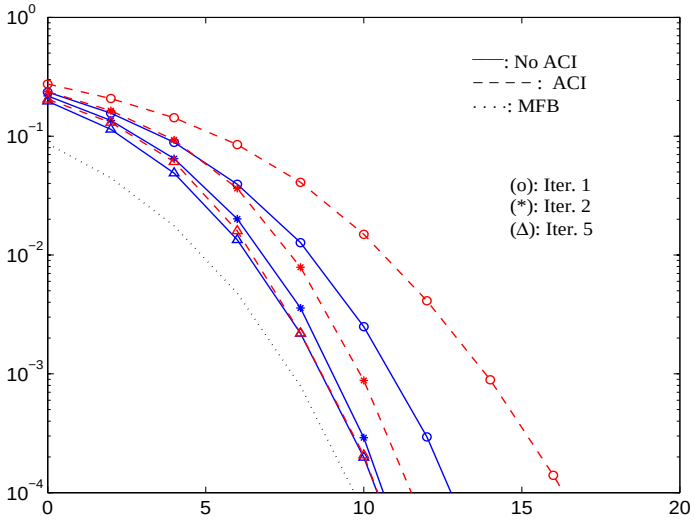

Fig. 8. Average BER performance for MSK signals with rectangular filtering with $B_T = 3R_S$.

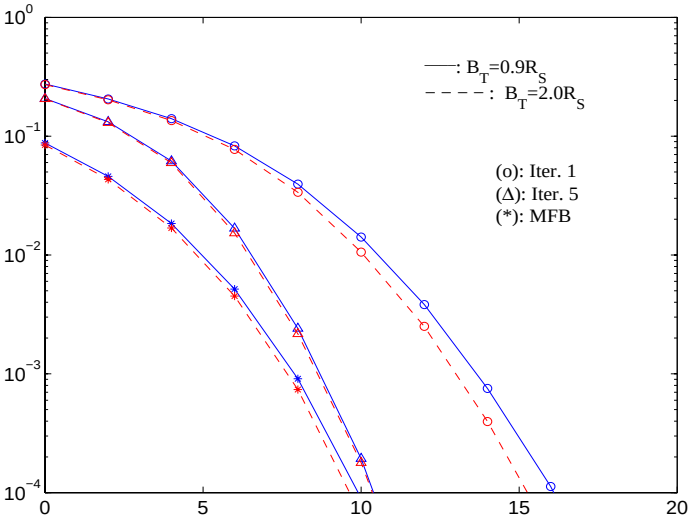

Fig. 10. Average BER performance for MSK signals with with Gaussian filtering and $\Delta f = R_S$ (i.e., with ACI).

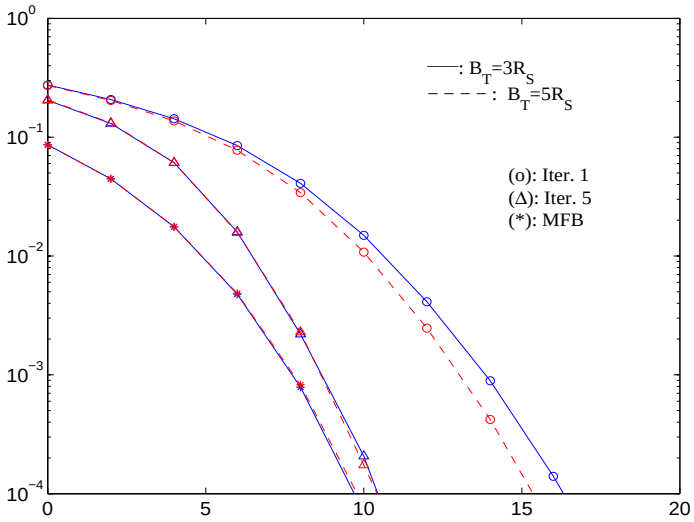

Fig. 9. Average BER performance for MSK signals with with rectangular filtering and $\Delta f = R_S$ (i.e., with ACI).

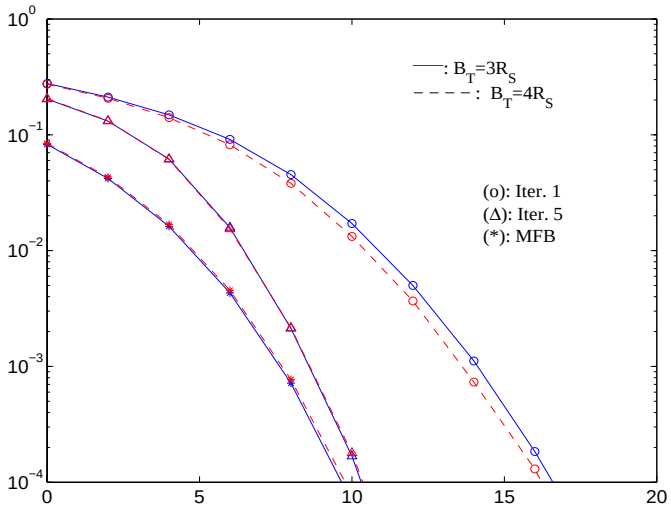

Fig. 11. Average BER performance for the modified pulses of fig. 4 with rectangular filtering and $\Delta f = R_S$ (i.e., with ACI).

VI. Conclusions

This paper considered SC-FDE systems employing OQPSK signals with quasi-constant envelope combined. Different frequency channels were separated by the symbol rate regardless of their bandwidth, allowing high spectral efficiency and we consider a frequency-domain receiver with ACI suppression. With this receiver it is possible to have high spectral efficiency with quasi-constant envelope OQPSK signals.

This technique is especially interesting for the uplink of future broadband wireless systems since we can employ low-cost, grossly nonlinear power amplifiers at the mobile terminals and almost all signal processing is shifted to the base station.

References

[1] A. Gusmão, R. Dinis, J. Conceição, and N. Esteves, "Comparison of Two Modulation Choices for Broadband Wireless Communications", *Proc. IEEE VTC Spring*, pp. 1300–1305, May 2000.

[2] D.Falconer, S.Ariyavisitakul, A.Benyamin-Seeyar and B.Eidson, "Frequency Domain Equalization for Single-Carrier Broadband Wireless Systems", *IEEE Comm. Mag.*, Vol. 4, No. 4, pp. 58–66, April 2002.

[3] R. Dinis, D. Falconer and B. Ng, "Iterative Frequency-Domain Equalizers for Adjacent Channel Interference Suppression", *IEEE GLOBECOM'05*, Dec. 2005.

[4] W. Gardner, *Introduction o Random Processes with Applications to Signals and Systems*, McGraw-Hill, 1990.

[5] W. Gardner, "Exploitation of Spectral Redundancy in Cyclostationary Signals", *IEEE Comm. Mag.*, Vol. 8, No. 2, pp. 14–36, Apr. 1991.

[6] B. Petersen and D. Falconer, "Suppression of Adjacent Channel, Co-channel, and Intersymbol Interference by Equalizers and Linear Combiners", *IEEE Trans. on Comm.*, Vol. 42, No. 12, pp. 3109–3118, Dec. 1994.

[7] A.Gusmão, P.Torres, R.Dinis and N.Esteves, "A Class of Iterative FDE Techniques for Reduced-CP SC-Based Block Transmission", *Int. Symposium on Turbo Codes*, April 2006.

[8] ETSI, "Channel models for HIPERLAN/2 in Different Indoor Scenarios", *ETSI EP BRAN 3ERI085B*, pp. 1-8, March 1998.